


Western North American Tree Populations Vulnerable to Climate Moisture Deficits

Volume 10 • Issue 8 | August 2022

Article

Identifying Western North American Tree Populations Vulnerable to Drought under Observed and Projected Climate Change

Kathryn Levesque and Andreas Hamann * 

Department Renewable Resources, University of Alberta, Edmonton, AB T6G 2H1, Canada; kathryn3@ualberta.ca
* Correspondence: andreas.hamann@ualberta.ca; Tel.: +1-(780)-492-6429

Abstract: Global climate change has affected forest health and productivity. A highly visible, direct climate impact is dieback caused by drought periods in moisture-limited forest ecosystems. Here, we have used a climate moisture index (CMI), which has been developed in order to map forest–grassland transitions, to investigate the shifts of the zero-CMI isopleths, in order to infer drought vulnerabilities. Our main objective was to identify populations of the 24 most common western North American forest tree species that are most exposed to drought conditions by using a western North American forest inventory database with 55,700 plot locations. We have found that climate change projections primarily increase the water deficits for tree populations that are already in vulnerable positions. In order to test the realism of this vulnerability assessment, we have compared the observed population dieback with changes in index values between the 1961–1990 reference period and a recent 1991–2020 average. The drought impacts that were predicted by negative CMI values largely conformed to the observed dieback in *Pinus edulis*, *Populus tremuloides*, and *Pinus ponderosa*. However, there was one notable counter-example. The observed dieback in the Canadian populations of *Populus tremuloides* were not associated with directional trends in the drought index values but were instead caused by a rare extreme drought event that was not apparently linked to directional climate change. Nevertheless, a macro-climatic drought index approach appeared to be generally suitable to identify and forecast the drought threats to the tree populations.

Keywords: drought; climate-moisture index; forests; aspen; ponderosa pine; pinyon pine; climate change; North America



Citation: Levesque, K.; Hamann, A. Identifying Western North American Tree Populations Vulnerable to Drought under Observed and Projected Climate Change. *Climate* **2022**, *10*, 114. <https://doi.org/10.3390/cli10080114>

Academic Editors: Jennifer A. Holm, David A. Lutz and Luxon Nhamo

Received: 30 May 2022

Accepted: 12 July 2022

Published: 29 July 2022

Publisher's Note: MDPI stays neutral with regard to jurisdictional claims in published maps and institutional affiliations.



Copyright: © 2022 by the authors. Licensee MDPI, Basel, Switzerland. This article is an open access article distributed under the terms and conditions of the Creative Commons Attribution (CC BY) license (<https://creativecommons.org/licenses/by/4.0/>).

1. Introduction

Tree growth and survival are strongly linked to their climatic environments, and for wide-ranging tree species, their local populations are also specialized to a set of environmental and climatic conditions that reflect the local adaptations to both the typical growing environments and rare extreme climate events [1]. As the climate changes, species, as well as their local populations, may no longer match their optimal climate niche [2]. The effects of this incompatibility can manifest as either a direct climate impact, or indirectly through biotic factors, such as changes in the competitive advantages relative to other species, or through vulnerability to pests and diseases [3]. Arguably, the most visible direct climate effects are dieback and the mortality that is caused by drought periods, while the most visible indirect effects are climate-related insect pests and disease outbreaks [4]. The less visible, yet important impacts include changes in the regenerative capacity and shifts in the relative competitive advantages among forest tree species [5,6]. As a result, the composition of forests is gradually altered.

Among the direct climate impacts, changes in the hydrological balance of forest ecosystems may be the most important driver of changes to the species demographics. Disruptions to the hydrological balance can be driven by a decrease in snowfall, earlier

spring melt and runoff, decreased precipitation during the growing season, and increased evapotranspiration that is driven by warmer temperatures [3,7]. The combined effects lead to the depletion of soil moisture reserves, which in turn compromise the photosynthesis rates and forest productivity [8]. For western North America, growth reductions, dieback, and mortality due to extreme drought events and gradual changes in the hydrological regimes have been widely documented [9–14], and the climate change projections from the latest CMIP6 multi-model ensembles show a consensus on further warming trends and a reduction in precipitation in the southwest of North America [15]. There is also evidence that climate change not only affects the most exposed populations at the southern- or low-elevation fringe of species distributions, but that locally-adapted populations throughout the range have varying physiological adaptive capacities and can therefore be affected by drought-related declines [16,17].

The direct climate effects often interact with additional biotic factors, amplifying the visible tree mortality. In western North America, unusual outbreaks of native pests and diseases have been linked to changes in the regional climate [18]. For instance, from 1989 to 2004, more than one million hectares of forest were killed by a spruce beetle outbreak in Alaska [19]. In British Columbia, more than 10 million hectares of lodgepole pine have been killed by the mountain pine beetle [20]. In the western United States, incidences of bark beetles and wood borer outbreaks have increased after drought periods [21]. An experimental study found that artificial drought stress made adult Colorado pine susceptible to bark beetle attacks and the subsequent mortality [22]. However, the relationship can be complex. Because some biotic pathogens thrive in moist environments while others are more successful in already stressed or moisture-deficit environments, it is difficult to predict the indirect drought impacts. For example, the geographic location, the insect type, and the primary and secondary fungal pathogens may interact in complex ways to affect the tree growth and mortality [21].

Nevertheless, drought stress remains to be a major driver of forest ecosystem vulnerability to climate change, justifying a focus on systematically evaluating the changes to the hydrological balance of tree populations at a macro-climatic scale. A useful metric for this purpose is Hogg's [23] climate moisture index (CMI). The CMI metric is conceptually similar to the Palmer drought severity index (PDSI), or the standardized precipitation evapotranspiration index (SPEI), in that it uses precipitation and temperature data to estimate a water balance, the given inflow through precipitation, and the outflow through evapotranspiration [24]. While the PDSI index is optimized for semi-arid climates and agricultural applications, taking the soil type, the soil recharge, and the runoff into account [25], the SPEI is a multiscale index that can be used across a wide range of climate regions, only requiring temperature and precipitation data [26]. The CMI metric uses the same approach to determine the water balances as SPEI, but uses an empirically-selected and optimized method to estimate the potential evapotranspiration for forest areas (modified Penman–Monteith), and is calibrated so that the zero-CMI isopleth for long-term climate normals predicts the forest distribution limits for western North America. Here, we investigate how the zero-CMI isopleth for the latest 30-year climate normal period (1991–2020) has shifted relative to the preceding climate normal (1961–1990), which serves as a useful reference period with a good station coverage for the climate conditions prior to a significant anthropogenic warming signal.

Because different species and their populations have different drought tolerances, this analysis will be carried out using a forest inventory plot database across western Canada and the United States, representing populations of the 24 most common species throughout their western North American range. Our main objective is to identify which tree species, and their populations, are exposed to drought conditions, with a secondary objective to validate the index-based predictions of drought vulnerability against the observed dieback and mortality. The specific objectives are (1) to determine individual species' CMI niche space; (2) to estimate the proportion of species populations that shift outside of each species' historic CMI niche space under the observed and projected climate change;

(3) to validate whether the CMI-inferred drought vulnerability under the observed climate change corresponds to the documented drought-related reductions in growth, dieback, or mortality.

2. Materials and Methods

The study relies on a compilation of 55,743 forest inventory plots of species occurrence for 24 western North American tree species, based on the Forest Inventory and Analysis (FIA) database of the U.S. Forest Service (<https://www.fia.fs.fed.us> accessed 15 September 2020), as well as additional records provided by provincial Canadian government agencies (compiled by Roberts and Hamann [27]). Some inaccuracies in the climatic characterizations of the plot locations of the FIA database could be caused by “fuzzing” and “swapping” of the location coordinates to protect the land owner’s privacy [28]. Because fuzzing does not affect elevation records, which we use for climate estimation, and swapping of plot location is only carried out within a county among plots with the highest ecological similarity, this should not have a large effect on our analysis.

Here, we use presence records for 24 tree species with the most records west of a 100-degree longitude. By region, the Pacific Northwest is represented by the following species: Pacific silver fir (*Abies amabilis*), noble fir (*Abies procera*), bigleaf maple (*Acer macrophyllum*), red alder (*Alnus rubra*), incense cedar (*Calocedrus decurrens*), Alaska yellow cedar (*Chamaecyparis nootkatensis*), Sitka spruce (*Picea sitchensis*), Douglas-fir (*Pseudotsuga menziesii*), coast redwood (*Sequoia sempervirens*), western red-cedar (*Thuja plicata*), and western hemlock (*Tsuga heterophylla*). Common species of the Cordilleras, interior plateau, and the Rocky Mountains include the following: lodgepole pine (*Pinus contorta*), mountain hemlock (*Tsuga mertensiana*), subalpine fir (*Abies lasiocarpa*), western larch (*Larix occidentalis*), western white pine (*Pinus monticola*), Engelmann spruce (*Picea engelmannii*), and whitebark pine (*Pinus albicaulis*); with ponderosa pine (*Pinus ponderosa*) and Colorado pine (*Pinus edulis*) having the most southerly distributions. Species with primarily boreal and sub-boreal distributions include white spruce (*Picea glauca*), black spruce (*Picea mariana*), paper birch (*Betula papyrifera*), and trembling aspen (*Populus tremuloides*).

To evaluate a macro-climatic scale water balance, we use Hogg’s [23] climate moisture index, which was specifically developed to track the forest–grassland transition at the zero-CMI isopleths. It is a monthly metric, which is calculated as precipitation minus potential evapotranspiration based on latitude and monthly temperature and precipitation. Aggregated over the course of the year, CMI values above zero indicate a positive annual evapotranspiration balance that supports forested ecosystems (in units of mm precipitation). Negative values indicate water deficits, with an expectation that forested ecosystems would not be supported. In this study, we focus on how CMI values for the latest 30-year climate normal period (1991–2020) have changed relative to the historic climate normal period (1961–1990), which often serves as a reference representing climate conditions before a significant anthropogenic warming signal.

For map visualizations, we generate interpolated climate grids of CMI at 1 km resolution. These climate grids were generated for the latest 30-year climate normal period (1991–2020) and the preceding historic climate normal period (1961–1990) with the ClimateNA software package v6.40a developed by Wang et al. [29] and available at <http://tinyurl.com/ClimateNA> (accessed 15 January 2021). Interpolated climate grids are based on the Parameter Regression of Independent Slopes Model (PRISM) interpolation method [30], and the software uses the delta method to generate monthly, annual, decadal, and 30-year normal time series data, based on Version 4 of the CRU-TS dataset [31] for particular locations and variables of interest. Future predictions are based on a 13-model ensemble of the Coupled Model Intercomparison Project phase 6 (CMIP6) of the World Climate Research Programme, using model selection criteria optimized for high-spatial but low-temporal resolution [15], as used in this study (1 km spatial resolution and 30 year climate normal projections). For the climatic characterization of plot locations, we use the location query tool of ClimateNA, which returns a lapse rate adjusted climate estimate,

using the reported elevation of the plot location. This elevation adjustment substantially improves the precision and accuracy of climate estimates [29].

To identify potentially threatened populations of species, we first assign percentiles to CMI values of plot locations for the 1961–1990 reference period for each species. The CMI value of the lowest 2.5 percentile of where the species occurs is used as a putative drought tolerance limit (although this is certainly not applicable for all species, as factors other than drought limit some species ranges, even at their driest extent). Subsequently, we calculate what additional proportion of plot locations for each species fall below the 2.5th percentile CMI value under observed climate change (1991–2020 climate normal), and under future projections, using a 13-model ensemble [15] for the 2020s, 2050s, and 2080s for the representative concentration pathways of 4.5 and 8.5.

3. Results

3.1. Climatology and Tree Cover of the Study Area

The climate that is suitable for tree cover in western North America comprises areas of high precipitation along the west coast and montane regions up to the tree line (Figure 1). In the interior boreal regions, the precipitation is low, but so is the temperature, leading to a positive evapotranspiration balance that supports the boreal forest. Generally, the climate moisture index (CMI) tracks the forest–grassland transition well, but there are notable exceptions. In the most southern regions, the CMI underpredicts the forest cover, most notably for the Sierras of Mexico. The under-prediction is less pronounced, but still notable, for the southern United States, for example in New Mexico (Figure 1). On the opposite end, the CMI overpredicts the forested regions in the high mountains and the high arctic. There, the tree growth is restricted by the cold temperatures and not by hydrological limitations. Generally, the CMI index works best to map the transition of temperate and boreal forests to prairie grasslands and shrub lands of the interior for western North America, for which it was designed [23].

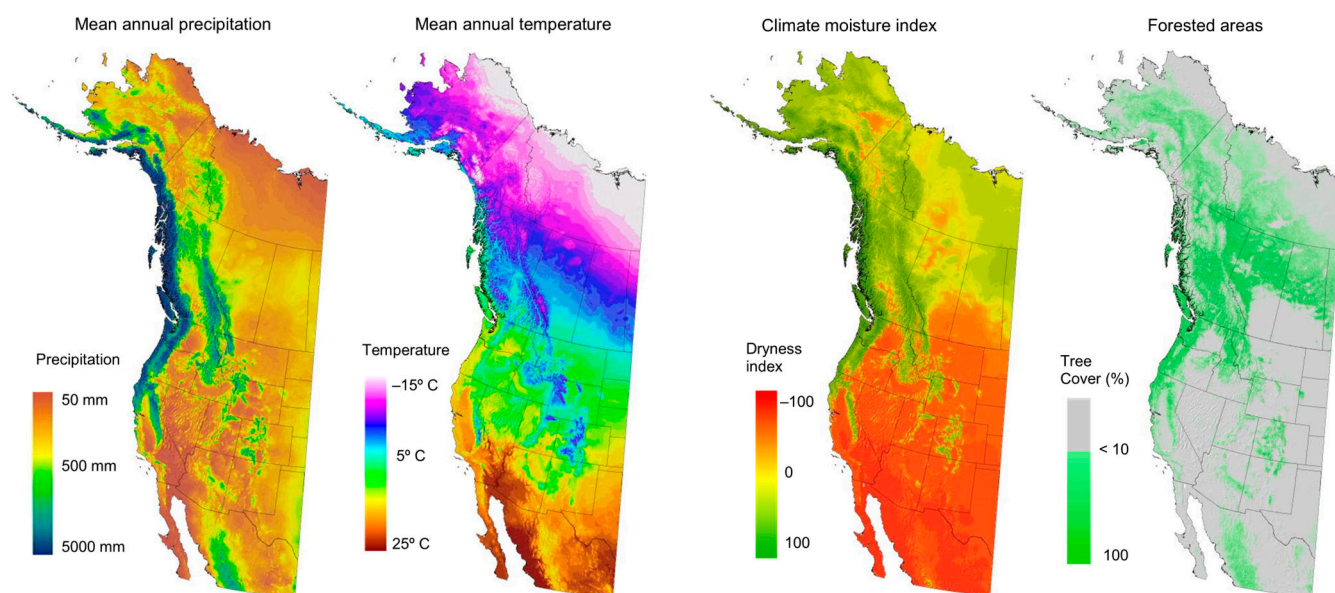


Figure 1. Climatology and tree cover of western North America. The climate moisture index (CMI) is estimated from precipitation, minus a latitude and temperature-driven monthly potential evapotranspiration estimate. Remotely-sensed tree cover (MODIS) approximately follows the CMI-inferred forest–grassland transition.

3.2. Observed and Projected Climate Change

The observed and projected climate change trends show some resemblance, but there are also major differences (Figure 2). Generally, the CMI projections from the atmosphere–ocean general circulation models (AOGCMs) suggest a shift towards higher water deficits across the sub-continent, except for the coast, Alaska, and the high mountain regions, with the most severe increase in water deficits in the south. In contrast, the observed changes also include areas of strong increases in water deficits for the eastern half of Alaska, the adjacent Yukon Territories, and the coastal areas of the Pacific Northwest. The observed shifts toward a more positive evapotranspiration balance for the period of 1990–2020 were observed for the coastal areas of California and the regions of the interior prairie grasslands (Figure 2). These changes are driven by the observed increases in temperature in the North and the reduced precipitation in Alaska, the coast of British Columbia, and the interior of California, Nevada, and New Mexico (See Appendix A, Figure A1 for a visualization of the combined effects of temperature and precipitation on CMI).

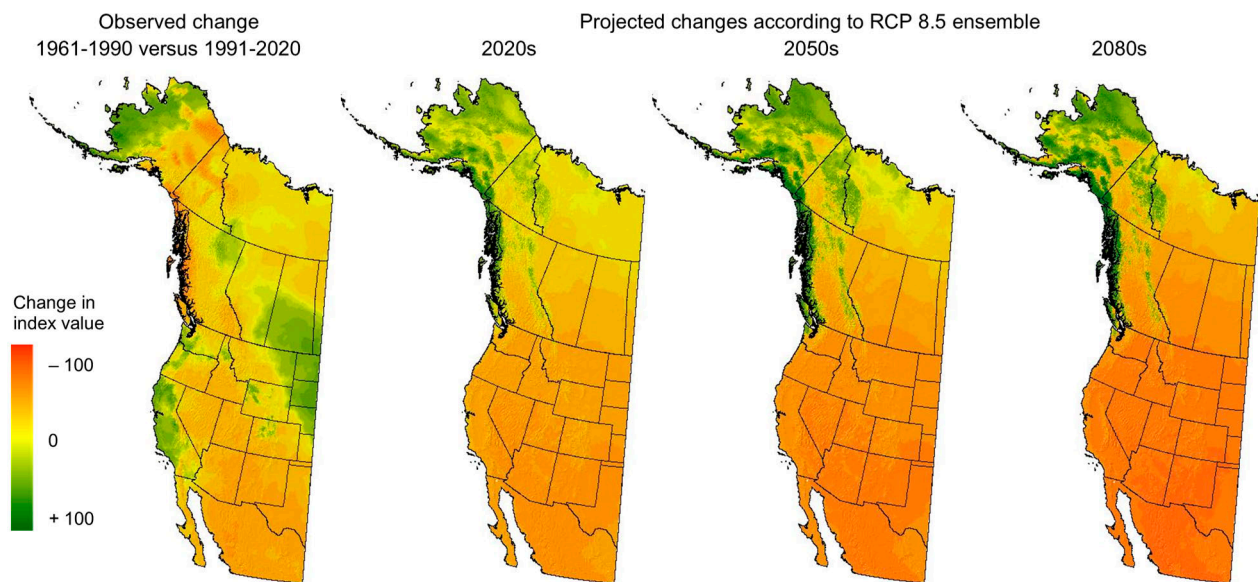


Figure 2. Observed and projected climate change, expressed through Hogg’s [23] climate moisture index (CMI). Observed changes are based on the CRU-TS v4 historical dataset [31], processed with the ClimateNA software package [29]. The projections shown are for a 13-model CMIP6 average ensemble [15], also included in the ClimateNA software. Changes in CMI as a combined effect of precipitation and temperature changes are visualized in Appendix A, Figure A1.

3.3. Drought Exposure of Tree Populations

In order to protect against outliers, we focus on the CMI values between the 2.5th and 97.5th percentile of the plot locations to describe the macro-climatic habitat where species occur, representing 95% of the occurrence records (Table 1). The most drought-tolerant western North American species, according to this metric, is the Colorado pine with CMI values of -96 to -23 , only occurring in habitats with strong annual water deficits (Table 1). Even the wettest habitat conditions where the Colorado pine occurs are too dry for most western North American species. Next, the Ponderosa pine, the interior Douglas-fir, and the incense cedar show strong drought tolerance limits, with 2.5th percentile CMI values of -69 , -42 , and -41 , respectively. All of these species border grasslands or shrub lands in the southern interior of western North America.

While the CMI metric is designed to model the forest–grassland transition at the zero-isopleth, many species have some populations within their distributions that are exposed to dry macro-climatic habitat conditions with negative CMI values. This includes boreal species at the southern edge of their distribution and tree species of the Pacific Northwest,

where species distribution limits occur along the rain shadows of the Coast Mountains, where the conditions become too dry. About half of the 24 species that were evaluated had 5% or more populations that were located in areas with negative CMI values, which are therefore potentially vulnerable to drought conditions (Table 1). Five species had 25% of their populations exposed to dry habitat, indicated by the CMI values below zero, and for two species, the Colorado pine and the ponderosa pine, half of the occurrence records were located within areas with negative CMI values.

Table 1. Climate moisture index values for the percentile of plot locations where each species occurs. We use the 2.5th percentile CMI value as a putative species drought tolerance metric for the purpose of subsequent analysis, although this should not be interpreted as a general species drought tolerance limit, as other climatic and non-climatic factors may limit species range. N denotes the number of presence records evaluated for each species.

Species	N	CMI Values for Percentiles of Species Presence Records										
		min	1	2.5	5	25	50	75	95	98	99	max
Colorado pine (<i>Pinus edulis</i>)	2836	−119	−103	−96	−92	−77	−67	−54	−31	−23	−13	20
Ponderosa pine (<i>Pinus ponderosa</i>)	3967	−98	−75	−69	−62	−40	−23	−4	44	70	94	270
Trembling aspen (<i>Populus tremuloides</i>)	7241	−53	−27	−19	−13	1	9	19	44	55	70	300
White birch (<i>Betula papyrifera</i>)	3926	−45	−20	−13	−7	2	10	23	62	81	102	297
White spruce (<i>Picea glauca</i>)	7115	−40	−13	−9	−5	4	14	25	55	69	88	190
Black spruce (<i>Picea mariana</i>)	2922	−13	−3	−1	2	10	18	27	48	57	73	146
Western larch (<i>Larix occidentalis</i>)	821	−42	−28	−26	−23	−1	15	37	85	108	123	167
Incense cedar (<i>Calocedrus decurrens</i>)	561	−56	−46	−41	−37	−5	24	61	124	167	198	290
Lodgepole pine (<i>Pinus contorta</i>)	11,275	−51	−19	−11	−4	14	27	48	107	162	291	532
Douglas-fir (<i>Pseudotsuga menziesii</i>)	8808	−79	−51	−42	−33	−7	16	61	186	228	280	509
Coast redwood (<i>Sequoia sempervirens</i>)	90	−31	−27	−22	−18	9	32	87	137	147	167	167
Subalpine fir (<i>Abies lasiocarpa</i>)	10,804	−45	−6	2	8	27	48	78	130	148	169	478
Engelmann spruce (<i>Picea engelmannii</i>)	6223	−48	−14	−6	1	32	57	86	129	145	164	213
Whitebark pine (<i>Pinus albicaulis</i>)	1038	−32	−8	9	17	41	66	92	135	151	168	294
Western white pine (<i>Pinus monticola</i>)	820	−53	−16	−9	0	37	70	114	224	287	356	380
Bigleaf maple (<i>Acer macrophyllum</i>)	437	−56	−47	−20	−2	49	86	129	213	237	268	278
Western redcedar (<i>Thuja plicata</i>)	3798	−40	−14	−5	4	34	91	191	350	387	443	606
Noble fir (<i>Abies procera</i>)	82	4	16	22	45	115	159	197	256	316	341	377
Red alder (<i>Alnus rubra</i>)	715	−41	13	29	46	99	137	213	320	349	379	553
Western hemlock (<i>Tsuga heterophylla</i>)	4860	−25	1	11	19	59	128	238	373	410	474	777
Pacific silver fir (<i>Abies amabilis</i>)	1615	−34	15	28	39	123	198	289	406	449	508	625
Mountain hemlock (<i>Tsuga mertensiana</i>)	1136	−28	24	46	61	113	185	279	424	498	577	777
Sitka spruce (<i>Picea sitchensis</i>)	1016	15	56	80	98	179	250	313	411	484	534	777
Yellow cedar (<i>Chamaecyparis nootkatensis</i>)	707	19	89	113	122	206	265	339	431	479	533	777

3.4. Vulnerable Populations under Observed and Projected Climate Change

The climate change projections suggest that water deficits will disproportionately increase for the species and populations that are already in vulnerable positions, whereas other species and populations are not predicted to be affected by the climate change impacts that are related to drought (Table 2). In ranking species vulnerabilities according to 2050's projections, the Colorado pine and the ponderosa pine are predicted to have the largest proportion of their current records shifted into climate conditions that are beyond their putative drought tolerance limit (i.e., the 2.5th percentile value from Table 1). In other words, the forested regions that are already water limited are projected to become drier and warmer at a faster rate than other regions in western North America that are wetter and cooler.

As a consequence, the species that rank near the top of Table 1, which occupy drier habitat conditions, will most likely have a larger proportion of their populations exposed to macro-climatic conditions beyond their tolerance limits (i.e., ranking high in Table 2). This negative relationship between the putative drought tolerance limit (i.e., the 2.5th percentile in Table 1) and the vulnerability under climate change holds true for both the projected climate change (Pearson correlation coefficient = -0.73 , $p < 0.001$) and the observed climate trends, as expressed by the difference in the 1961–1990 normals compared to the 1991–2020 normals ($r = -0.61$, $p < 0.001$). The relationship remains significant, even with the Colorado pine removed, which drives the correlation for the observed climate impacts ($r = -0.47$, $p < 0.05$).

Table 2. Percentage of plot locations that additionally fall below the 2.5th percentile threshold shown in Table 1 under observed and projected climate change.

Species	Observed	Projection 2020s		Projection 2050s		Projection 2080s	
		RCP 4.5	RCP 8.5	RCP 4.5	RCP 8.5	RCP 4.5	RCP 8.5
Colorado pine (<i>Pinus edulis</i>)	3.1	16.5	17.5	39.6	60	52.7	84.8
Ponderosa pine (<i>Pinus ponderosa</i>)	0	7.2	7.2	14.4	24.3	20.8	42.5
Western larch (<i>Larix occidentalis</i>)	−0.4	6.8	7.6	12.5	17.8	16.4	34
Incense cedar (<i>Calocedrus decurrens</i>)	−0.4	7.5	8.2	13.4	17.6	15.5	24.1
Black spruce (<i>Picea mariana</i>)	1.1	5	5.3	9.9	17	15.6	43.5
Douglas–fir (<i>Pseudotsuga menziesii</i>)	−0.3	3.4	3.7	7.1	11.1	9.7	21.4
Trembling aspen (<i>Populus tremuloides</i>)	0.4	3.9	4.3	7.2	10.3	9.1	23.9
Coast redwood (<i>Sequoia sempervirens</i>)	−1.4	1.9	4.2	7.5	9.7	8.6	11.9
Lodgepole pine (<i>Pinus contorta</i>)	0.2	3.3	3.6	6	8.5	7.7	18.5
Subalpine fir (<i>Abies lasiocarpa</i>)	0.3	2.7	3	5.4	7.8	6.9	17.1
Whitebark pine (<i>Pinus albicaulis</i>)	−0.8	3.4	3.8	5.9	7.7	7	13.8
Engelmann spruce (<i>Picea engelmannii</i>)	−0.1	3.1	3.3	5.1	7.4	6.4	13.8
White birch (<i>Betula papyrifera</i>)	1	2.5	2.5	4.9	7.1	6.3	21.6
White spruce (<i>Picea glauca</i>)	0.4	1.9	1.9	3.8	6.9	6.3	26.9
Western white pine (<i>Pinus monticola</i>)	−0.7	2.4	2.9	4.6	5.9	5.4	12.1
Western redcedar (<i>Thuja plicata</i>)	0.7	1.8	2.1	3.9	5.6	4.7	10.9
Western hemlock (<i>Tsuga heterophylla</i>)	−1.2	2	2.1	3.2	4.4	4	7.6
Bigleaf maple (<i>Acer macrophyllum</i>)	−0.7	1.6	1.8	2.5	3.2	2.8	7.8
Amabilis fir (<i>Abies amabilis</i>)	−1.9	2.1	2.1	2.3	2.7	2.6	3.6
Red alder (<i>Alnus rubra</i>)	−1.9	1	1	1.7	2.5	1.8	4.8
Noble fir (<i>Abies procera</i>)	−0.1	2.4	2.4	2.4	2.4	2.4	3.6
Mountain hemlock (<i>Tsuga mertensiana</i>)	−2.4	0.8	1	1.5	2.3	1.9	4.3
Yellow cedar (<i>Chamaecyp. nootkatensis</i>)	−0.5	0.5	0.5	0.9	1	0.8	1.2
Sitka spruce (<i>Picea sitchensis</i>)	−2.5	0.3	0.3	0.4	0.6	0.4	1.3

Therefore, the observed climate change impacts conform in direction, while not yet in magnitude, to the future projections. The 1991–2020 observed climate normals represent the 2000’s projections (mid-decade), while the 2020’s projections in Table 2 correspond to the 2011–2030 AOGCM average ensemble. Over the next decades, we would expect significantly more drought impacts on a large number of western North American forestry species, if the projections hold true and the CMI index values that we have used in this study are a useful representation of species drought tolerances.

4. Discussion

In order to discuss the realism of the CMI-based drought vulnerability assessment, we compared the observed dieback and mortality reports from the scientific literature with CMI-inferred drought vulnerability from this study (Figure 3). The most notable drought-related dieback and mortality in western North America that has been observed over the last three decades has been reported for the aspen (*Pinus tremuloides*), the Colorado pine (*Pinus edulis*), and, to a lesser degree, the ponderosa pine (*Pinus ponderosa*) [10,12,14,22,32–42]. This corresponds to the top three most drought-exposed populations of common western-North American tree species, as described by Hogg’s CMI metric (Table 1). The individual populations that are below the 2.5th percentile of the CMI values under the 1961–1990 climate period (Table 1) are shown in Figure 3. The CMI-inferred vulnerable populations partly correspond to the regions of observed dieback, but not in all cases.

Aspen experienced widespread mortality, dieback, reduced growth, and tent caterpillar infestations of trees that were weakened by drought conditions [10,12,14,38–42]. The CMI-inferred vulnerable populations correspond well to areas of aspen decline, which were comprehensively reported by Worrall et al. [42]. The notable exception is a false-positive prediction of the CMI-inferred population vulnerabilities in the southern interior of British Columbia (Figure 3, cluster of red dots without a documented mortality region), and a false-negative prediction for Alberta and Saskatchewan, where widespread aspen decline has been documented [10,12,39,42], but no populations were predicted to cross the 2.5th percentile CMI value for the 1991–2020 period.

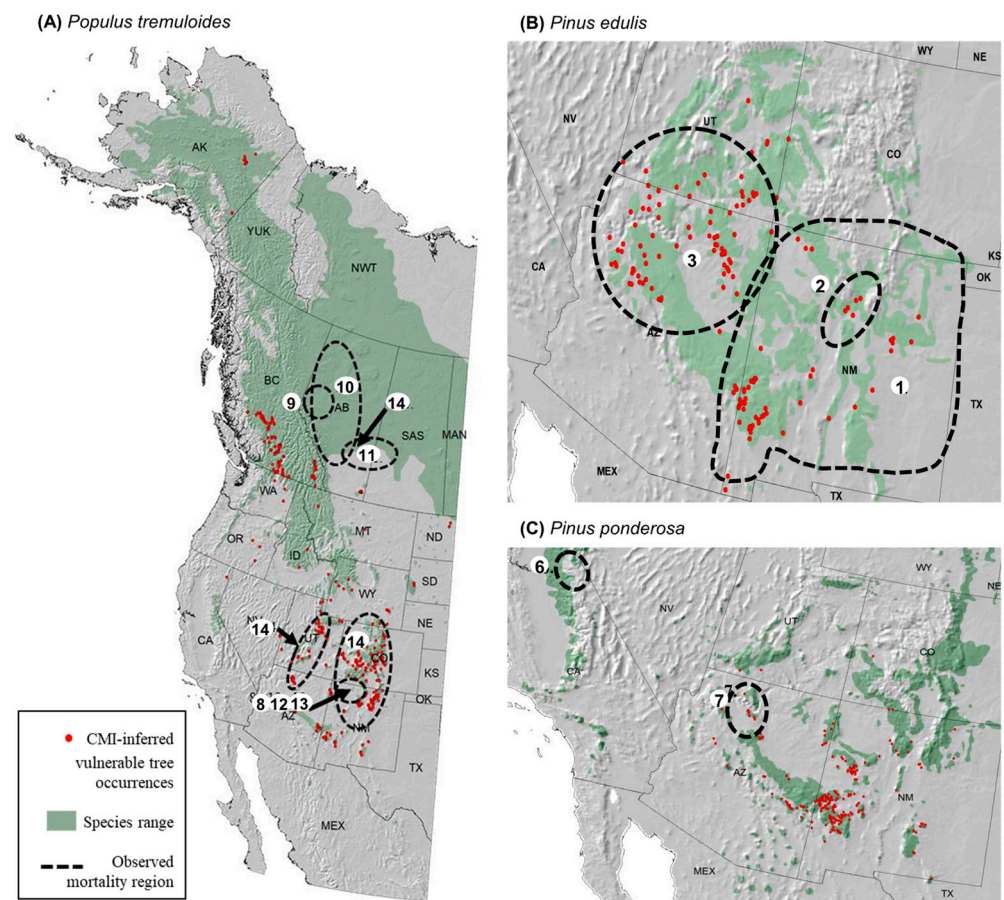


Figure 3. Plot locations identified as potentially vulnerable to drought based on a climate moisture index (CMI) versus documented dieback and mortality for three forest tree species: (A) aspen, (B) Colorado pine, and (C) ponderosa pine. Numbers refer to reference IDs that document the drought impacts [10,12,14,22,32–42], listed in Appendix B, Table A1.

This highlights an important limitation of the CMI metric in the way we have used it here. By comparing consecutive 30-year normal periods, we have intentionally focused on the long-term directional climate trends. In contrast, the mortality and dieback are almost always caused by extreme climate events, such as high-severity 2-year drought events. While a shift in means makes the extreme events more likely, they still occur randomly. In this case, a severe drought occurred in Alberta in 2000–2002, while the long-term trend toward drier conditions was more severe in British Columbia (Figure 2, left panel). In fact, the portions of the boreal grassland–forest transition zone where aspen dieback occurred in Alberta and Saskatchewan (Figure 3A, Region 11) experienced a long-term trend toward wetter conditions (Figure 2, green shades in the corresponding area).

For the Colorado pine, the CMI-inferred vulnerabilities are a simple true-positive at the species level (Figure 3B). With a relatively restricted range, and almost the entire range affected by drought, a population-level evaluation in the case of the aspen was not possible. The species receives the highest CMI-inferred vulnerability score for its natural range (Table 1), and for its observed and projected vulnerability (Table 2), by a large margin. The species is also the most thoroughly documented case of drought-related decline and mortality among western North American tree species [22,32–35], which was, in some cases, exacerbated by bark beetles, but with drought being a dominant stressor that predisposes these trees to infestations [35].

The observed drought impacts for the Ponderosa pine occurred primarily in California and Arizona (Figure 3C). As in the case of the aspen, the CMI-inferred drought vulnerability did not yield vulnerable species populations that crossed the 2.5th percentile threshold of the CMI values in California. In fact, we found a long term-trend toward slightly wetter conditions when comparing the consecutive 30-year normal periods (Figure 2, left panel, yellow and green shades indicating a neutral trend toward wetter conditions). Nevertheless, extreme drought events in the 1996–2007 period did occur in both California and Arizona, which caused up to 74% mortality of the ponderosa pine, also insect pest mediated, during the 2002–2007 timeframe [18,36,37].

5. Conclusions

This study shows that overall species-level exposure, according to the CMI-metric (Table 1), appears to be a reliable indicator of species vulnerability to drought conditions. The impacts that were predicted by negative CMI values largely conformed to observed dieback in the aspen (*Pinus tremuloides*), the Colorado pine (*Pinus edulis*), and the ponderosa pine (*Pinus ponderosa*). This suggests that the metric should also be useful at the population level, but the random nature of when and where extreme drought events occur make specific local predictions of population decline more difficult. Notably, the observed dieback in the Canadian populations of aspen was not associated with directional trends in the drought index values but was instead caused by a rare extreme drought event that was not linked to directional climate change. Nevertheless, it appears to be inevitable that more western North American species will experience declines and mortality due to direct drought-related climate change impacts if the projections for the 2050s and 2080s become reality (Table 2). In addition to the species that are already impacted, the western larch (*Larix occidentalis*), the white spruce (*Picea glauca*), and the paper birch (*Betula papyrifera*) are expected to experience major issues, based on the positioning of their populations on the continental CMI gradient and the climate change projections for the following decades. The black spruce (*Picea mariana*) may be protected by occurring primarily in water-logged habitats, but two species of major ecological and economic importance, the Douglas-fir (*Pseudotsuga menziesii*) and the lodgepole pine (*Pinus contorta*), are predicted to be negatively impacted by the drought conditions that are expected under climate change over the next decades.

Author Contributions: The research project was conceived by A.H. and K.L. conducted the analysis and generated the figures and tables. A.H. provided the funding, advice, and contributed data and analysis tools. K.L. wrote a first draft of the manuscript, which was edited by A.H. All authors have read and agreed to the published version of the manuscript.

Funding: This research was funded by a Discovery Grant of the Natural Sciences and Engineering Research Council of Canada (NSERC), grant number RGPIN-330527-20.

Institutional Review Board Statement: Not applicable.

Informed Consent Statement: Not applicable.

Data Availability Statement: Plot data used in this study is publicly available through the Forest Inventory and Analysis (FIA) Program of the U.S. Forest Service, and directly from the provincial government agencies of Canada upon request.

Conflicts of Interest: The authors declare no conflict of interest. The funders had no role in the design of the study; in the collection, analyses, or interpretation of data; in the writing of the manuscript, or in the decision to publish the results.

Appendix A

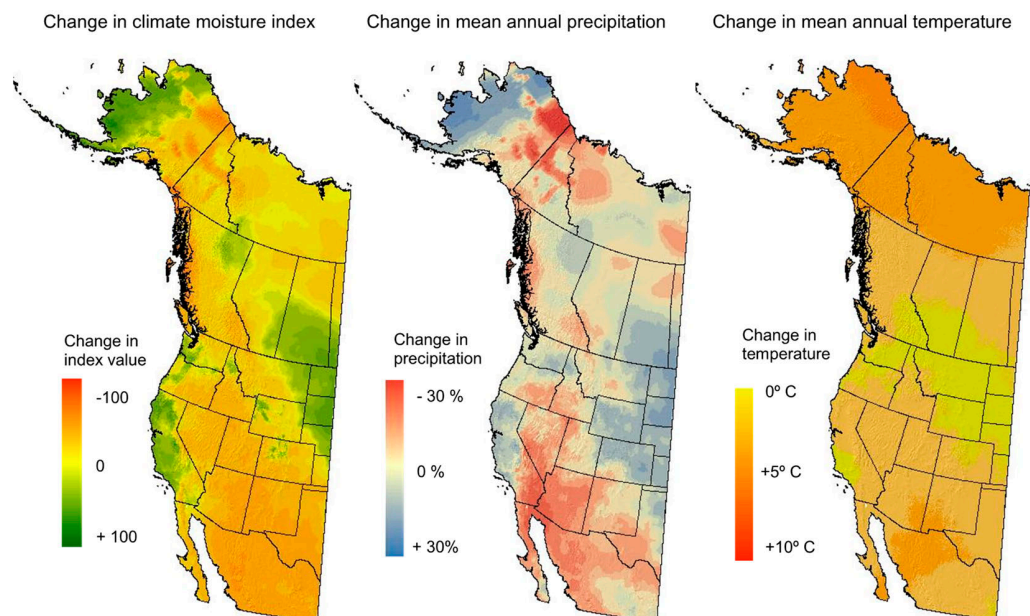


Figure A1. Change in climate moisture index values in the context of underlying changes in precipitation and temperature across western North America. The maps are based on the CRU-TS 4.05 database [31] and were processed through the ClimateNA software package [29]. For all three variables, the maps represent the difference between the 1961–1990 historic climate normal period and the most recent 1991–2020 climate normal.

Appendix B

Table A1. References and brief synopsis of observed dieback and mortality of three western North American tree populations. The ID field corresponds to locations shown in Figure 3.

ID	Region	Impact and severity synopsis
<i>Colorado pine (Pinus edulis)</i>		
1	NM	Clifford et al. [32] reports 42% of the Colorado pine forests within the study region classified as die-off (1029 km ²) with an increasing mortality gradient from south to north. Mortality occurred primarily in areas receiving less than 600mm in precipitation.
2	NM	Gaylord et al. [22] found that drought predisposes Colorado pine stands to lead to insect attacks. Mortality due to insect attacks was higher in water deprived sites.
3	AZ, CO, ID, MT, NV, NM, UT, and WY	Shaw et al. [33] reports idespread mortality in Colorado pine associated with several years of drought in the southwestern United States. The combined effects of drought, insects, and disease cause mortality approaching 100% in some areas.
4	NM	Breshears et al. [34] found that smaller less severe droughts preceded a major drought in 2000–2003. Mortality caused by water stress ws related to the depletion of carbon reserves, also creating susceptibility to insect attacks. Mortality affected 12,000 km ² in New Mexico with mortality rates up to 90% based on remote sensing.
5	CO, NM, AZ	Floyd et al. [35] documents mortality rates of 32–65% for Colorado pine in southwest Colorado, northern New Mexico, and northern Arizona, with ips beetles primarily responsible for mortality on trees predisposed by severe drought conditions.
<i>Ponderosa pine (Pinus ponderosa)</i>		
6	CA	Byer and Jin [37] report approximately 20% mortality of ponderosa pine in a remote sensing survey of the Central and Southern Sierra Nevada following a 2012–2016 drought period. High mortality rates were associated with high forest density and low elevation areas.
7	AZ	Ganey and Voita [36] observed mortality of ponderosa present at 98% of sites (1 ha/site) between 2002–2007, following a 1997–2002 drought period, representing an average increase of 74% over baseline mortality. Mortality was precipitated by insect infestation, following severe drought conditions.

Table A1. Cont.

ID	Region	Impact and severity synopsis
Trembling aspen (<i>Populus tremuloides</i>)		
8	CO	Anderegg et al. [38] investigate hydraulic changes in surviving trees from a 2000–2003 drought period, documenting an increased vulnerability to future drought events.
9	AB	Hogg et al. [39] document growth reductions and insect infestations associated with historical drought periods using tree ring analysis. Aspen dieback during 1990–1992 and growth reductions were primarily explained by tent caterpillar defoliation, climate moisture index from the previous year, growing degree days, and snow depth in order of importance.
10	Western Canada	Chen et al. [12] link reduced growth of aspen in a plot network across western Canada to droughts effects. Both temporal and spatial variation in growth reductions were explained by a standardized precipitation–evapotranspiration index (SPEI).
11	AB and SK	Michaelian et al. [10] document massive mortality of aspen following severe drought in 2001–2002 along the southern edge of the Canadian boreal forest. Aerial surveys revealed extensive patches of severe mortality (>55%) resembling the impacts of fire. Dead aboveground biomass was estimated at 45 Mt, representing 20% of the total aboveground biomass.
12	CO	Huang and Anderegg [14] report large drought-induced aboveground live biomass losses in southern Rocky Mountain aspen forests. Of 60 sites, 30% experienced greater than 50% canopy dieback, 57.9% were affected by aspen mortality, and above ground biomass loss was estimated as 30.7% representing 2.7 Tg of carbon emissions.
13	CO	Worrall et al. [41] document aspen mortality (mean 32%) across 56,000 ha in southwestern Colorado. Primary mortality agents were canker, bark beetles, and borers. Predisposition of climatic factors were inferred from high mortality being associated with low elevation, and southern and western aspects.
14	Western North America	Worrall et al. [42] linked declines of <i>Populus tremuloides</i> in North America linked to climate. Drought was identified as a significant factor in this period of decline, and a bioclimate envelope model confirmed that dieback and mortality corresponded to loss of climatic habitat for the study period.
15	Canadian Boreal	Peng et al. [40] documented drought-induced increase in tree mortality across Canada's boreal forests. Western boreal seen more severe mortality rates than the east. Annual increases in mortality for aspen increased from less than 1% to 2.5% per year on average from the 1960s to 2000s.

References

- Morgenstern, E.K. *Geographic Variation in Forest Trees: Genetic Basis and Application of Knowledge in Silviculture*; The University of British Columbia Press: Vancouver, CA, USA, 1996; 209p.
- Aitken, S.N.; Yeaman, S.; Holliday, J.A.; Wang, T.L.; Curtis-McLane, S. Adaptation, migration or extirpation: Climate change outcomes for tree populations. *Evol. Appl.* **2008**, *1*, 95–111. [[CrossRef](#)] [[PubMed](#)]
- Chmura, D.J.; Anderson, P.D.; Howe, G.T.; Harrington, C.A.; Halofsky, J.E.; Peterson, D.L.; Shaw, D.C.; St Clair, J.B. Forest responses to climate change in the northwestern United States: Ecophysiological foundations for adaptive management. *For. Ecol. Manag.* **2011**, *261*, 1121–1142. [[CrossRef](#)]
- Allen, C.D.; Macalady, A.K.; Chenchouni, H.; Bachelet, D.; McDowell, N.; Vennetier, M.; Kitzeberger, T.; Rigling, A.; Breshears, D.D.; Hogg, E.T. A global overview of drought and heat-induced tree mortality reveals emerging climate change risks for forests. *For. Ecol. Manag.* **2010**, *259*, 660–684. [[CrossRef](#)]
- Morin, X.; Fahse, L.; Jactel, H.; Scherer-Lorenzen, M.; Garcia-Valdes, R.; Bugmann, H. Long-term response of forest productivity to climate change is mostly driven by change in tree species composition. *Sci. Rep.* **2018**, *8*, 5627. [[CrossRef](#)] [[PubMed](#)]
- Zhang, T.; Niinemets, U.; Sheffield, J.; Lichstein, J.W. Shifts in tree functional composition amplify the response of forest biomass to climate. *Nature* **2018**, *556*, 99–102. [[CrossRef](#)]
- Vicente-Serrano, S.M.; Quiring, S.M.; Pena-Gallardo, M.; Yuan, S.S.; Dominguez-Castro, F. A review of environmental droughts: Increased risk under global warming? *Earth-Sci. Rev.* **2020**, *201*, 102953. [[CrossRef](#)]
- Reich, P.B.; Sendall, K.M.; Stefanski, A.; Rich, R.L.; Hobbie, S.E.; Montgomery, R.A. Effects of climate warming on photosynthesis in boreal tree species depend on soil moisture. *Nature* **2018**, *562*, 263–267. [[CrossRef](#)]
- van Mantgem, P.J.; Stephenson, N.L.; Byrne, J.C.; Daniels, L.D.; Franklin, J.F.; Fule, P.Z.; Harmon, M.E.; Larson, A.J.; Smith, J.M.; Taylor, A.H.; et al. Widespread Increase of Tree Mortality Rates in the Western United States. *Science* **2009**, *323*, 521–524. [[CrossRef](#)]
- Michaelian, M.; Hogg, E.H.; Hall, R.J.; Arsenault, E. Massive mortality of aspen following severe drought along the southern edge of the Canadian boreal forest. *Glob. Chang. Biol.* **2011**, *17*, 2084–2094. [[CrossRef](#)]
- Hogg, E.H.; Michaelian, M.; Hook, T.I.; Undershultz, M.E. Recent climatic drying leads to age-independent growth reductions of white spruce stands in western Canada. *Glob. Chang. Biol.* **2017**, *23*, 5297–5308. [[CrossRef](#)]
- Chen, L.; Huang, J.G.; Alam, S.A.; Zhai, L.H.; Dawson, A.; Stadt, K.J.; Comeau, P.G. Drought causes reduced growth of trembling aspen in western Canada. *Glob. Chang. Biol.* **2017**, *23*, 2887–2902. [[CrossRef](#)] [[PubMed](#)]
- Goulden, M.L.; Bales, R.C. California forest die-off linked to multi-year deep soil drying in 2012–2015 drought. *Nat. Geosci.* **2019**, *12*, 632–637. [[CrossRef](#)]

14. Huang, C.-Y.; Anderegg, W.R.L. Large drought-induced aboveground live biomass losses in southern Rocky Mountain aspen forests. *Glob. Chang. Biol.* **2012**, *18*, 1016–1027. [[CrossRef](#)]
15. Mahony, C.R.; Wang, T.L.; Hamann, A.; Cannon, A.J. A global climate model ensemble for downscaled monthly climate normals over North America. *Int. J. Clim.* **2022**, *early view*. [[CrossRef](#)]
16. Montwe, D.; Isaac-Renton, M.; Hamann, A.; Spiecker, H. Drought tolerance and growth in populations of a wide-ranging tree species indicate climate change risks for the boreal north. *Glob. Chang. Biol.* **2016**, *22*, 806–815. [[CrossRef](#)] [[PubMed](#)]
17. Isaac-Renton, M.; Montwe, D.; Hamann, A.; Spiecker, H.; Cherubini, P.; Treydte, K. Northern forest tree populations are physiologically maladapted to drought. *Nat. Commun.* **2018**, *9*, 5254. [[CrossRef](#)] [[PubMed](#)]
18. Anderegg, W.R.L.; Hicke, J.A.; Fisher, R.A.; Allen, C.D.; Aukema, J.; Bentz, B.; Hood, S.; Lichstein, J.W.; Macalady, A.K.; McDowell, N.; et al. Tree mortality from drought, insects, and their interactions in a changing climate. *New Phytol.* **2015**, *208*, 674–683. [[CrossRef](#)]
19. Berg, E.E.; Henry, J.D.; Fastie, C.L.; De Volder, A.D.; Matsuoka, S.M. Spruce beetle outbreaks on the Kenai Peninsula, Alaska, and Kluane National Park and Reserve, Yukon Territory: Relationship to summer temperatures and regional differences in disturbance regimes. *For. Ecol. Manag.* **2006**, *227*, 219–232. [[CrossRef](#)]
20. Kurz, W.A.; Dymond, C.C.; Stinson, G.; Rampley, G.J.; Neilson, E.T.; Carroll, A.L.; Ebata, T.; Safranyik, L. Mountain pine beetle and forest carbon feedback to climate change. *Nature* **2008**, *452*, 987–990. [[CrossRef](#)]
21. Kolb, T.E.; Fettig, C.J.; Ayres, M.P.; Bentz, B.J.; Hicke, J.A.; Mathiasen, R.; Stewart, J.E.; Weed, A.S. Observed and anticipated impacts of drought on forest insects and diseases in the United States. *For. Ecol. Manag.* **2016**, *380*, 321–334. [[CrossRef](#)]
22. Gaylord, M.L.; Kolb, T.E.; Pockman, W.T.; Plaut, J.A.; Yezpez, E.A.; Macalady, A.K.; Pangle, R.E.; McDowell, N.G. Drought predisposes pinon-juniper woodlands to insect attacks and mortality. *New Phytol.* **2013**, *198*, 567–578. [[CrossRef](#)] [[PubMed](#)]
23. Hogg, E.H. Temporal scaling of moisture and the forest-grassland boundary in western Canada. *Agric. For. Meteorol.* **1997**, *84*, 115–122. [[CrossRef](#)]
24. Keyantash, J.; Dracup, J.A. The quantification of drought: An evaluation of drought indices. *Bull. Am. Meteorol. Soc.* **2002**, *83*, 1167–1180. [[CrossRef](#)]
25. Heim, R.R. A review of twentieth-century drought indices used in the United States. *Bull. Am. Meteorol. Soc.* **2002**, *83*, 1149–1165. [[CrossRef](#)]
26. Vicente-Serrano, S.M.; Begueria, S.; Lopez-Moreno, J.I. A Multiscalar Drought Index Sensitive to Global Warming: The Standardized Precipitation Evapotranspiration Index. *J. Clim.* **2010**, *23*, 1696–1718. [[CrossRef](#)]
27. Roberts, D.R.; Hamann, A. Method selection for species distribution modelling: Are temporally or spatially independent evaluations necessary? *Ecography* **2012**, *35*, 792–802. [[CrossRef](#)]
28. Gray, A.N.; Brandeis, T.J.; Shaw, J.D.; McWilliams, W.H.; Miles, P.D. Forest Inventory and Analysis Database of the United States of America (FIA). *Biodivers. Ecol.* **2012**, *4*, 225–231. [[CrossRef](#)]
29. Wang, T.L.; Hamann, A.; Spittlehouse, D.; Carroll, C. Locally Downscaled and Spatially Customizable Climate Data for Historical and Future Periods for North America. *PLoS ONE* **2016**, *11*, e0156720. [[CrossRef](#)]
30. Daly, C.; Halbleib, M.; Smith, J.I.; Gibson, W.P.; Doggett, M.K.; Taylor, G.H.; Curtis, J.; Pasteris, P.P. Physiographically sensitive mapping of climatological temperature and precipitation across the conterminous United States. *Int. J. Clim.* **2008**, *28*, 2031–2064. [[CrossRef](#)]
31. Harris, I.; Osborn, T.J.; Jones, P.; Lister, D. Version 4 of the CRU TS monthly high-resolution gridded multivariate climate dataset. *Sci. Data* **2020**, *7*, 109. [[CrossRef](#)]
32. Clifford, M.J.; Royer, P.D.; Cobb, N.S.; Breshears, D.D.; Ford, P.L. Precipitation thresholds and drought-induced tree die-off: Insights from patterns of *Pinus edulis* mortality along an environmental stress gradient. *New Phytol.* **2013**, *200*, 413–421. [[CrossRef](#)] [[PubMed](#)]
33. Shaw, J.D.; Steed, B.E.; DeBlander, L.T. Forest Inventory and Analysis (FIA) annual inventory answers the question: What is happening to pinyon-juniper woodlands? *J. For.* **2005**, *103*, 280–285.
34. Breshears, D.D.; Cobb, N.S.; Rich, P.M.; Price, K.P.; Allen, C.D.; Balice, R.G.; Romme, W.H.; Kastens, J.H.; Floyd, M.L.; Belnap, J.; et al. Regional vegetation die-off in response to global-change-type drought. *Proc. Natl. Acad. Sci. USA* **2005**, *102*, 15144–15148. [[CrossRef](#)]
35. Floyd, M.L.; Clifford, M.; Cobb, N.S.; Hanna, D.; Delph, R.; Ford, P.; Turner, D. Relationship of stand characteristics to drought-induced mortality in three Southwestern pinon-juniper woodlands. *Ecol. Appl.* **2009**, *19*, 1223–1230. [[CrossRef](#)]
36. Ganey, J.L.; Vojta, S.C. Tree mortality in drought-stressed mixed-conifer and ponderosa pine forests, Arizona, USA. *For. Ecol. Manag.* **2011**, *261*, 162–168. [[CrossRef](#)]
37. Byer, S.; Jin, Y.F. Detecting Drought-Induced Tree Mortality in Sierra Nevada Forests with Time Series of Satellite Data. *Remote Sens.* **2017**, *9*, 929. [[CrossRef](#)]
38. Anderegg, W.R.L.; Plavcova, L.; Anderegg, L.D.L.; Hacke, U.G.; Berry, J.A.; Field, C.B. Drought's legacy: Multiyear hydraulic deterioration underlies widespread aspen forest die-off and portends increased future risk. *Glob. Chang. Biol.* **2013**, *19*, 1188–1196. [[CrossRef](#)]
39. Hogg, E.H.; Brandt, J.P.; Kochtubajda, B. Growth and dieback of Aspen forests in northwestern Alberta, Canada, in relation to climate and insects. *Can. J. For. Res.* **2002**, *32*, 823–832. [[CrossRef](#)]
40. Peng, C.H.; Ma, Z.H.; Lei, X.D.; Zhu, Q.; Chen, H.; Wang, W.F.; Liu, S.R.; Li, W.Z.; Fang, X.Q.; Zhou, X.L. A drought-induced pervasive increase in tree mortality across Canada's boreal forests. *Nat. Clim. Chang.* **2011**, *1*, 467–471. [[CrossRef](#)]

41. Worrall, J.J.; Egeland, L.; Eager, T.; Mask, R.A.; Johnson, E.W.; Kemp, P.A.; Shepperd, W.D. Rapid mortality of *Populus tremuloides* in southwestern Colorado, USA. *For. Ecol. Manag.* **2008**, *255*, 686–696. [[CrossRef](#)]
42. Worrall, J.J.; Rehfeldt, G.E.; Hamann, A.; Hogg, E.H.; Marchetti, S.B.; Michaelian, M.; Gray, L.K. Recent declines of *Populus tremuloides* in North America linked to climate. *For. Ecol. Manag.* **2013**, *299*, 35–51. [[CrossRef](#)]